Definition of an N-Terminal Actin-binding Domain and a C-Terminal Ca^{2+} Regulatory Domain in Human Brevin

Joseph Bryan and Shuying Hwo

Department of Cell Biology, Baylor College of Medicine, Houston, Texas 77030

Abstract. Brevin is a Ca^{2+}-modulated actin-associated protein that will sever F-actin and cap barbed filament ends. Limited proteolysis with chymotrypsin or subtilisin cleaves the molecule approximately in half. Cleavage is ~10-fold more rapid in Ca^{2+} than in EGTA. The two fragments are readily separated from each other and from undigested brevin by high pressure liquid chromatography on a DEAE resin. A 40,000-mol-wt fragment from the N-terminal is not retained by DEAE, while a 45,000-mol-wt C-terminal fragment binds more tightly than brevin. The N-terminal fragment retains ~10% of the nucleation activity, caps barbed ends, and retains 50% of the total severing activity defined by dilution induced depolymerization of pyrenyl actin, but, in contrast to brevin, none of these functions are affected by Ca^{2+}. Fluorescent actin binding studies and gel-filtration demonstrate that the 40,000-mol-wt fragment binds two actin monomers. The 45,000-mol-wt C-terminal fragment has no severing, nucleating, or capping activity. Cross-reaction with two monoclonal antibodies against two specific Ca^{2+}-induced conformations of human platelet gelsolin suggest that both Ca^{2+} binding sites are located on the carboxyl half of the brevin molecule. One epitope, defined as the rapidly exchanging Ca^{2+} binding site in the gelsolin–actin complex, is lost when a 20,000-mol-wt fragment is cleaved from the carboxyl terminal. The second epitope, related to the poorly exchanging Ca^{2+} binding site in the complex, is nearer the middle of the brevin molecule.

GELSOLIN and a similar plasma protein called brevin (4–8, 15, 18, 20, 23) show Ca^{2+}-modulated interactions with G and F-actin. Gelsolin has two Ca^{2+} binding sites (3, 24) and two actin-binding sites (3). Brevin has similar properties (4, and unpublished data). Under non-polymerizing conditions, gelsolin will form a tight complex with two actin monomers and two calcium ions. Lowering the Ca^{2+} concentration with EGTA reduces the affinity for one actin and one Ca^{2+}. These can then be removed by gel filtration or centrifugation. The other actin molecule and Ca^{2+} ion are trapped on gelsolin (3) or brevin and can be isolated as a complex. The estimated half-time for dissociation of the brevin–actin–Ca^{2+} complex in EGTA is ~30–35 d (Sedlar, P. A., and J. Bryan, unpublished data). We have arbitrarily termed the non-exchangeable site as site I and distinguish an actin site I and a Ca^{2+} site I from their more rapidly exchanging site II counterparts. Gelsolin will sever F-actin filaments (2, 11, 20, 25), will nucleate the assembly of G-actin (11, 14, 17, 20, 21), and cap barbed filament ends (2, 20, 21). Which sites are involved in severing and capping is not yet clear. Recently we have demonstrated that the gelsolin–actin complex, GA_1CA_2, with actin site I occupied will cap, but not sever actin filaments, and have presented evidence that free gelsolin (GCa_2) does not readily cap barbed ends (2). In this paper we begin to explore the inter-relationships between actin and Ca^{2+} sites I and II and relate these to capping and severing activities using protease digestion and conformation specific monoclonal antibodies.

We have defined two monoclonal antibodies against human platelet gelsolin that recognize conformational changes induced by Ca^{2+} binding (9). 4F8 IgA appears to recognize an epitope induced when the non-exchangeable site (I) is occupied; 8G5 IgG appears to recognize an epitope induced when the exchangeable site (II) is occupied. We demonstrate here that human brevin has a protease-sensitive region near the middle of the molecule. Subtilisin and chymotrypsin both cleave Ca^{2+} liganded brevin to produce two fragments with apparent molecular weights of ~40,000 and 45,000. The two fragments can be readily separated by DEAE chromatography. The 40-kD fragment is less acidic and elutes before brevin, whereas the 45-kD fragment is more tightly bound to DEAE. The actin binding activity is on the 40-kD fragment, which is derived from the amino terminal half of the protein. The 40-kD fragment retains a large fraction of the original severing activity, but proteolytic cleavage of the parent molecule eliminates the Ca^{2+} sensitivity of the filament severing reaction. The Ca^{2+}-induced epitopes are both on the 45-kD fragment from the carboxyl half of the molecule.The 4F8 epitope is nearer the center of the molecule, whereas the 8G5 epitope is on a terminal 20-kD fragment at the carboxyl end.

Materials and Methods

Protein Purification

Brevin was immunopurified from pooled human sera following the procedures outlined in Hwo and Bryan (9). Monoclonal antibodies were isolated from serum-free harvest fluid. The purification and characterization of 4F8 IgA and 8G5 IgG are given in Hwo and Bryan (9). Actin was prepared according to Spudich and Watt (16) and labeled with pyrene iodoacetamide as described by Bryan and Coluccio (2). Protein determinations were done by the method of Bradford (1). The brevin concentration was estimated using an extinction coefficient of 150,000/M per cm determined for bovine brevin (10).

Fluorescence Measurements

Dilution induced depolymerization experiments using pyrene F-actin were done as described by Bryan and Coluccio (2). Actin monomer binding was measured using NBD(nitrobenzoxadiazole)[1]–actin as described by Bryan and Kurth (3). Pyrene actin excitation and emission wavelengths were 365 and 407 nm, respectively; NBD–actin excitation and emission wavelengths were 475 and 530 nm, respectively.

SDS Gel Electrophoresis and Immunoblotting

SDS gel electrophoresis was done as outlined by Laemmli (13). Immunoblots were performed as described by Towbin et al. (19) modified as described by Hwo and Bryan (9).

Sequencing of Peptides

A model 470A gas phase sequencer (Applied Biosystems, Inc., Foster City, CA) was used for all analyses. PTH amino acids were identified by high pressure liquid chromatography (HPLC) using a Beckman model 344 chromatograph equipped with two model 112 pumps and two model 160 detectors (Beckman Instruments, Inc., Palo Alto, CA). Samples were automatically injected using a model M710B Waters Intelligent Sample Processor (WISP, Waters Instruments, Rochester, MN). PTH amino acids were analyzed using a 5-μm pore size IBM cyano column (4.5 mm × 25 cm) (IBM Instruments, Inc., Danbury, CT) with either a DuPont ETH guard column or a pellicular CN guard column (DuPont Co., Wilmington, DE). The samples were analyzed at 35°C using a gradient system that consisted of buffer A (0.02 M sodium acetate, 5% tetrahydrofuran, pH 5.95 and 17 μl of HPLC grade acetone/liter) and buffer B (acetonitrile). The PTH amino acids are eluted by increasing buffer B from 11% to 45% at 2% per minute at a flow rate of 1 ml/min.

HPLC Fractionation

Brevin and brevin digests were fractionated using a Waters HPLC apparatus. DEAE chromatography was done on a Waters DEAE-5PW column, 0.75 × 7.5 cm. The flow rate was 1 ml/min. The solvent was 25 mM Tris-HCl, pH 7.0. 0.1 mM EGTA. A gradient from 0 to 0.4 M NaCl was developed over 30 min; 0.5-ml fractions were collected and analyzed for protein by Bradford assay (1), by SDS gel electrophoresis, and using various functional assays as described in the text.

Gel filtration was done using Waters Protein Pak 300SW and ^{125}I gel-filtration columns in tandem. 10–50-μl samples at 0.5–2 mg/ml were injected. The flow rate was 1 ml/min. The solvent was 0.1 M sodium phosphate, pH 7.0. The columns were calibrated using various molecular weight standards, which include beta-galactosidase, 520,000; ferritin, 440,000; catalase, 232,000; phosphorylase, 94,000; bovine serum albumin (BSA), 67,000; ovalbumin, 43,000 and carbonic anhydrase, 30,000.

Protease Cleavage

Brevin at 1 mg/ml was cleaved with bacterial subtilisin (type VII, Sigma Chemical Co., St. Louis, MO) or *N*α-*p*-tosyl-L-lysine chloromethyl ketone–treated chymotrypsin (type VII, Sigma Chemical Co.) using various conditions as indicated in the figure legends. The buffer used was 10 mM Tris-HCl, 0.5 mM $CaCl_2$, 1 mM NaN_3, pH 8.0 at a temperature of 20°C. The reaction was stopped by addition of EGTA to 1 mM and diisopropylfluorophosphate (DIFP) to 5 mM. The DIFP was stored as a 200 mM stock solution in propylene glycol at −20°C.

[1] *Abbreviations used in this paper:* DIFP, diisopropylfluorophosphate; HPLC, high pressure liquid chromatography; NBD, nitrobenzoxadiazole.

Results

The results of one experiment in which brevin was digested with subtilisin at a weight ratio of 1:100 enzyme/brevin are shown in Fig. 1 *a*. At early times the two major cleavage products are S45 and S40, 45- and 40-kD polypeptides, respectively. These are then cleaved into two slightly smaller polypeptides; S45 yields S44 and S40 yields S38. We see similar results (Fig. 1 *b*) using chymotrypsin at 1:100 enzyme/brevin (wt/wt) concentrations. Cleavage products, CT45 and CT40, are produced at early digestion times that have molecular weights ~45,000 and 40,000. At later times the 45-kD fragment is cleaved to a 43–44-kD fragment, and the 40-kD fragment is cleaved to pieces with apparent molecular mass of ~30 and 15 kD. Ca^{2+} liganded brevin is more accessible to both subtilisin and chymotrypsin. For comparison, the partial results from one experiment using chymotrypsin in the presence of EGTA are also shown in Fig. 1 *c*. Comparing the extent of hydrolysis at various times, we estimate that Ca^{2+} liganded brevin is about 10 times more sensitive to proteolysis than the unliganded form. Experiments using BSA as the protease substrate show that neither chymotrypsin nor subtilisin have intrinsic calcium sensitivity.

Immunoblotting with 4F8 IgA and 8G5 IgG shows that the epitopes recognized by both monoclonal antibodies are on the 45/43-kD fragments. Selected lanes from the gels in Fig. 1 are shown in Fig. 2. More pronounced proteolysis by subtilisin generates smaller fragments of S44 each of which has only one of the epitopes. S34 is the smallest fragment we have identified that binds to 4F8 IgA, and S37 is the smallest that is recognized by 8G5 IgG (data not shown). Monoclonal antibody binding to all of the fragments is strictly dependent upon the presence of calcium.

Fig. 2 shows data that place the 8G5 epitope on one end of the brevin molecule. In some preparations we see a proteolytic fragment with a molecular weight of ~70,000–75,000. This fragment cross-reacts strongly with 4F8 IgA, but not with 8G5 IgG, indicating that the 8G5 epitope is on the missing 20-kD fragment.

Separation of Brevin Fragments by DEAE-Chromatography

Brevin and the 40- and 45/43-kD fragments are readily separated by DEAE-chromatography. Fig. 3 *a* shows the resolution of a chymotrypsin digest of 3 mg of brevin. CT40 is not retained by the DEAE column in 25 mM Tris-HCl, 0.1 mM EGTA, pH 7.4 at 2.5–5 min. Brevin elutes at 0.19 M at ~29–30 min, and CT45/43 elutes at 0.24 M NaCl at ~34 min. The results suggest that one half of the brevin molecule, the 45-kD fragment, is considerably more acidic than the other half. Fig. 3 *b* illustrates the purity of the three major peaks and shows the cross-reactivity with the two monoclonal antibodies.

Sequence Data

We have placed the 40-kD fragment on the amino half of the parent brevin molecule by sequencing a small fraction of S38 which is derived from this polypeptide. The results are shown in Scheme I. The S38 sequence begins with residue 24 of brevin (22). For this sequencing we used a preparation that

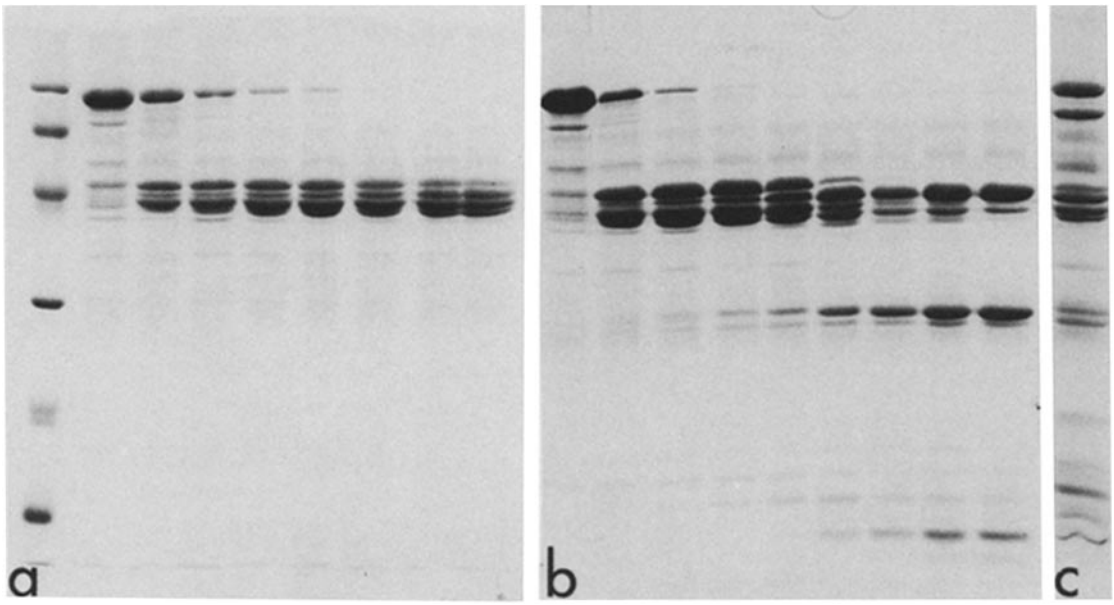

Figure 1. Proteolysis of brevin. Panel *a* illustrates the digestion of human brevin using bacterial subtilisin at a 1:100 wt/wt ratio. The enzyme was added and the reaction stopped by addition of EGTA to 1 mM and DIFP to 5 mM at various times. The first lane contains marker proteins with known molecular weights; phosphorylase b, 94,000; BSA, 67,000; ovalbumin, 45,000; carbonic anhydrase, 30,000; soybean trypsin inhibitor, 21,000; and lysozyme, 14,300. The digestion times were 0, 5, 10, 15, 20, 30, 45, and 60 min in lanes *2–9*, respectively. There is an accumulation of four peptides. Panel *b* illustrates a similar digestion using chymotrypsin at a 1:100 wt/wt ratio. From left-to-right the reaction times were 0, 1, 3, 5, 10, 30, 60, 90, and 120 min. At early times we see predominately two peptides with apparent molecular weights of 40,000 and 45,000. The 45,000 species gives rise to a third peptide at 43,000; the 40,000 species gives rise to one at about 38,000 that is progressively degraded to fragments of ~30,000–31,000 and 15,000. Panel *c* shows a 120-min digestion time point with chymotrypsin in the presence of EGTA. Compare with the last lane in *b*. Solution conditions: 10 mM Tris-HCl, 0.5 mM $CaCl_2$, 1 mM NaN_3, pH 8.0 for the digestions in *a* and *b*. The digestion in *c* was done in the same buffer plus 2 mM EGTA. The brevin concentration was 1 mg/ml in each digestion mixture; the temperature was 20°C.

was greater than 90% pure S38. Although we have not sequenced S40, we make the tentative conclusion that S38 is generated from S40 by cleavage at residue 24.

Activity of Cleaved Products

To estimate the activity of the fragments relative to intact brevin, we have compared the severing activity of brevin with an unfractionated mixture of polypeptides from a subtilisin digest equivalent to the 30-min time point shown in Fig. 1 *a*, lane *7*. The results are shown in Fig. 4 *a*. Equal amounts of brevin were present in the digested and undigested samples. A 20-μl aliquot of pyrene–F-actin at 3 μM was diluted into 1,500 μl of 100 mM KCl, 3 mM $MgCl_2$, 0.5 mM ATP, 2 mM Tris-HCl, pH 8, to a final actin concentration of 40 nM. The EGTA samples contained 1 mM EGTA; the Ca^{2+} samples contained 0.2 mM $CaCl_2$. The brevin samples contained 1 nM undigested brevin; the digested samples contained an equivalent amount of digested brevin. In the presence of Ca^{2+}, brevin markedly increases the rate of depolymerization (open triangles). This effect is attenuated 8-to-9-fold in EGTA (closed triangles) and closely resembles the control without added brevin (circles). The digested brevin retains a substantial severing activity in Ca^{2+} (open squares) and shows no modulation upon reducing the Ca^{2+} concentration (filled squares). It is difficult to quantitate the severing activity precisely, but the initial rate of depolymerization with digested brevin is approximately one-half that of the parent molecule. A similar result is seen for nucleation. Fig. 4 *b* shows the results of initiating assembly of 5 μM actin (5% pyrene-labeled actin, 95% unlabeled actin) in the presence of 50 nM brevin or an equivalent amount of digested brevin. The degree of brevin digestion was equivalent to that used in the severing experiment. Brevin nucleates rapid assembly in the presence of Ca^{2+} (open triangles) and, under these conditions, slows assembly in the presence of EGTA (closed triangles). Digested

```
                                                    10
Brevin  ALA-THR-ALA-SER-ARG-GLY-ALA-SER-GLN-ALA-
                                                    20
        GLY-ALA-PRO-GLN-GLY-ARG-VAL-PRO-GLU-ALA-
        XXX-PRO-ASN-
                                                    30
Brevin                  XXX-MET-VAL-VAL-GLU-HIS-PRO-GLU-PHE-LEU-LYS-ALA-
S38                     XXX-MET-VAL-VAL-GLU-XXX-PRO-GLU-PHE-XXX-LYS-ALA.
```

Scheme I. Comparison of amino terminal sequence for brevin and S38.

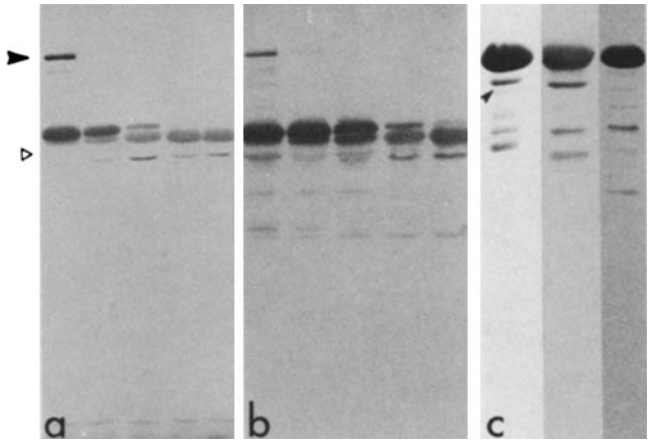

Figure 2. Cross-reactivity of brevin fragments with conformation-specific monoclonal antibodies. Panels *a* and *b* show immunoblots stained using 8G5 IgG and 4F8 IgA, respectively. The gels are from lanes *3–7* of the chymotrypsin digest shown in Fig. 1 *b*. Both antibodies recognize the 45,000- and 43,000-mol-wt fragments, but not the 40,000-mol-wt fragment, whose position is indicated by the open arrow. Lane *1* in *c* shows the Coomassie Blue profile of a brevin preparation with a 75,000-mol-wt peptide, U75, marked by the small arrow, that is produced by an unknown protease in our preparations. This peptide reacts strongly with 4F8 IgA in lane *2, c*, but not with 8G5 IgG in the last lane. We infer that the 8G5 epitope is on a 15,000–20,000-mol-wt piece at one end of the brevin molecule. The larger arrowhead marks the position of the parent brevin molecule.

brevin shows some nucleation in both Ca^{2+} and EGTA with no apparent modulation. The initial rate of assembly of the samples with digested brevin was 10–12% of the control brevin rate in calcium. Both the digested and undigested molecules appear to cap the barbed filament ends as shown by a reduction in the final fluorescence values. The effective nucleation by the brevin digest is strongly dependent upon the concentration used. At low concentrations, less than 1 digested brevin per 100–200 actin molecules, we see a decrease in the rate of assembly compared with controls, similar to that observed with gelsolin and gelsolin–actin complexes (11). We interpret this as capping of some of the barbed ends with an apparent decrease in the overall rate of polymerization. Higher concentrations of the active fragment(s) increase the apparent rate of assembly above the control rate. The control polymerization curve in EGTA has been omitted for clarity, but lies between the brevin plus Ca^{2+} curve and the brevin digest values.

Identification of the Major Severing Fragment

The severing activity of the DEAE purified chymotryptic fragments is shown in Fig. 5. The open circles show the depolymerization of the control F-actin diluted to 40 nM. Intact brevin at 1.5 nM in the presence of Ca^{2+} increases the rate of depolymerization ~25-fold (open triangles), but has little effect in EGTA (data not shown). The 40-kD fragment, at 1.5 nM, increases the rate of depolymerization ~12-fold (open squares), about one-half the value for brevin. The activity of the purified 40-kD fragment shows no attenuation in 1–10 mM EGTA (filled squares). The 45/43-kD piece has no detectable effect at 15 nM, 10 times the concentration of the 40-kD fragment as shown by the closed circles that are equivalent to control values.

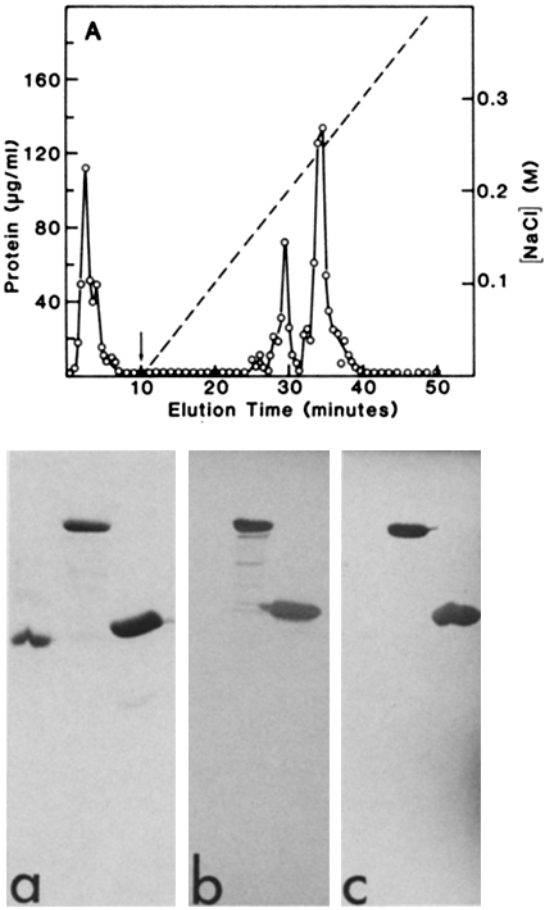

Figure 3. Fractionation of a brevin digest by DEAE ion-exchange chromatography. 3 mg of brevin were digested with 30 μg of chymotrypsin for 10 min at 20°C. The reaction was stopped by addition of EGTA to 1 mM and DIFP to 5 mM. The brevin concentration was 6 mg/ml in 10 mM Tris-HCl, 0.5 mM $CaCl_2$, pH 8.0 with 1 mM NaN_3. The sample was applied to a Waters DEAE-5PW column and eluted with a NaCl gradient of 0.01 M/min. The flow rate was 1 ml/min. 0.5-ml fractions were collected and analyzed for protein using the Bradford assay. The protein profile is shown in *a*. Three major fractions were observed corresponding, as shown in *b* in order of elution, to the 40-kD protein, brevin, and the 45-kD protein. Fig. 3 *b*, panel *a* shows the Coomassie Blue staining profiles for the 2.5-, the 29.5-, and the 34-min fractions. Panel *b* shows the same fractions blotted with 4F8 IgA, and panel *c* shows the same fractions blotted with 8G5 IgG.

Identification and Characterization of Actin Binding Fragments

We have used three approaches to identify and characterize further the half of the molecule that binds actin: chromatography of digests on DNAse I-Sepharose, reconstitution of fragments with actin followed by gel-filtration, and enhancement of NBD–actin fluorescence. Chromatography on DNAse I was done by adding G-actin to the DIFP-inactivated digestion mixture at 2 mol of actin per mole of brevin, incubating for 30 min at 4°C, and chromatographing on DNAse I-agarose as described by Wang and Bryan (20). The 45/43-kD fragments, from either a subtilisin or a chymotrypsin digest, are not retained at high or low ionic strength, in the presence or absence of calcium, or in the presence or absence of magnesium. An EGTA wash, which normally

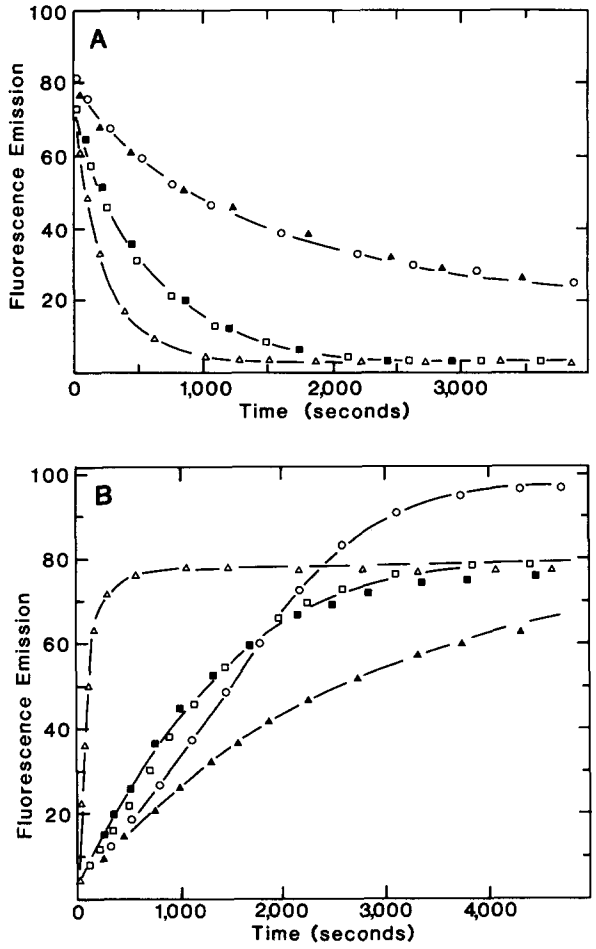

Figure 4. Assay of the severing and capping activities of brevin proteolytic digests. The activity of a 30-min subtilisin digest equivalent to that shown in lane 7 of Fig. 1 *a* was assayed for its effects on dilution induced depolymerization of F-actin (*a*) and on G-actin polymerization (*b*). In *a*, the effect of 1 nM brevin in $CaCl_2$ (△) or EGTA (▲) is compared with either 1 nM digested brevin in $CaCl_2$ (□), in EGTA (■) or with buffer alone (○). The initial rates are ~0.045, 0.16, and 0.32 fluorescence units s^{-1} for control or brevin in EGTA, for brevin digests, and for brevin in $CaCl_2$, respectively. In each experiment, 3 μM pyrene actin, 100% labeled, was diluted to a final concentration of 40 nM into 2 mM Tris-HCl, 100 mM KCl, 3 mM $MgCl_2$, 0.5 mM ATP, 0.2 mM $CaCl_2$ at pH 8.0 plus the added proteins. The EGTA samples also had 2 mM EGTA. In *b*, 5 μM G-actin, 5% pyrene-labeled, was assembled by addition of KCl to 100 mM and $MgCl_2$ to 3 mM in the presence of digested or undigested brevin and either 0.2 mM $CaCl_2$ or 2 mM EGTA. ○, control assembly in 0.2 mM $CaCl_2$; △, undigested brevin in 0.2 mM $CaCl_2$; ▲, undigested brevin in 0.2 mM $CaCl_2$ plus 2 mM EGTA; □, digested brevin in 0.2 mM $CaCl_2$; and ■, digested brevin in 0.2 mM $CaCl_2$ plus 2 mM EGTA. The control assembly in 0.2 mM $CaCl_2$ plus 2 mM EGTA is omitted for clarity, but lies between the brevin plus Ca^{2+} data and the 40-kD fragment values. The brevin concentration, either digested or undigested, was 50 nM. The temperature was 20°C.

removes gelsolin–actin (20) or brevin–actin complexes (Bryan, J., and S. Hwo, unpublished data), does not remove protein. Actin and 40-kD fragments are released using either 3 M quanidine-HCl or 0.1 M glycine-HCl, pH 2.8. We conclude that the 40-kD fragment is the actin binding half of the brevin molecule. After either quanidine or low pH treatment, the actin can be separated from the 40-kD fragment by

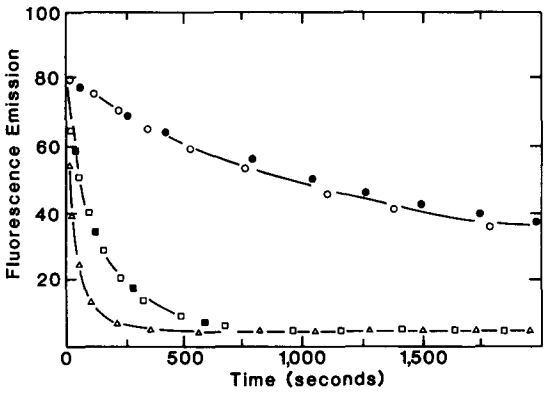

Figure 5. The amino terminal half of the brevin molecule severs F-actin and is not Ca^{2+} regulated. The severing activity of the DEAE purified 40- and 45-kD fragments was assayed as described in Fig. 4 *a*. The results for the 40-kD fragment from the amino terminal, at 1.5 nM, are shown by the squares. □, data from an experiment using 0.2 mM $CaCl_2$; ■, data obtained using 0.2 mM $CaCl_2$ plus 2 mM EGTA. We see no difference plus or minus Ca^{2+}. △, brevin control data, 1.5 nM, plus 0.2 mM $CaCl_2$. The brevin control data plus EGTA have been omitted for clarity, but fall on the F-actin control depolymerization curve (○). ●, data for depolymerization in 15 nM of the 45-kD fragment from the carboxyl terminal in 0.2 mM $CaCl_2$. The results in 2 mM EGTA are equivalent. The solution conditions are the same as those given in Fig. 4 *a*.

dialysis to lower the salt concentration followed by chromatography on DEAE-Sephacel or on DEAE using HPLC as shown in Fig. 3. Depolymerization experiments show that S40 or CT40 purified by actin–DNAse I and DEAE chromatography severs F-actin about as efficiently as the DEAE purified material (data not shown).

Number of Actin Binding Sites on the 40-kD Fragment

Reconstitution experiments give a more quantitative estimate of the number of actin molecules bound per 40-kD fragment. We have shown previously that an NBD–actin bound at actin site I on gelsolin has the same fluorescence quantum yield as NBD–G-actin, but an NBD–actin bound at actin site II has approximately a 2.5 times greater quantum yield similar to NBD–F-actin (3). Fig. 6 *a* shows a titration curve for brevin in the presence of 0.2 mM $CaCl_2$. An extrapolation of a least squares line through the first three data points to the intercept with a horizontal line through the plateau gives a value of 1.8 molecules of actin bound per molecule of brevin. Fig. 6 *b* shows the normalized binding curves for brevin and the 40-kD fragment in both Ca^{2+} and EGTA. The brevin and 40-kD protein values were determined by the Bradford dye binding assay or using the extinction coefficient for bovine brevin (10). The curves for both brevin and the 40-kD fragment are quite similar; the striking difference is that the 40-kD–actin interaction is not Ca^{2+} regulated. A similar extrapolation of the initial binding data for the 40-kD fragment gives a value of 2.4 actin molecules bound/40-kD fragment. The reasons for the somewhat higher value are unclear, but could be due to differences in dye binding or extinction coefficient for the whole versus part of the molecule.

Complex formation was also examined using HPLC gel filtration. The results for CT45/43 are summarized in Fig. 7 *a*. We see no evidence for actin–45/43-kD fragment inter-

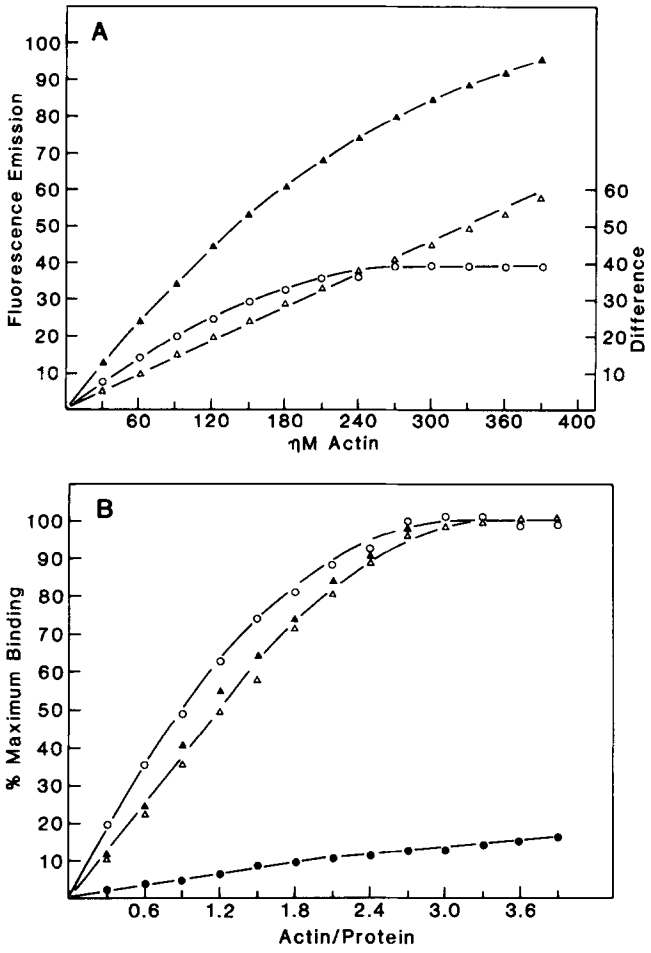

Figure 6. Titration of actin-binding sites on brevin and the 40-kD fragment using NBD-actin. (*a*) Titration of 100 nM brevin with NBD-actin. Aliquots of NBD-actin in 2 mM Tris-HCl, 0.2 mM $CaCl_2$, 0.5 mM ATP at pH 8.0 were added to 100 nM brevin in the same buffer plus 2 mM $MgCl_2$ (▲) or to the buffer alone (△). The brevin samples show a fluorescence increase equivalent to that described previously for gelsolin (3). The difference binding curve is given by the open circles and shows saturation at ~1.8 actin molecules per brevin. For a different preparation of brevin this estimate has a range of 1.8–2.2 actin molecules/brevin. (*b*) Binding data for brevin and the 40-kD fragment are compared. The 40-kD fragment gives an extrapolated value of 2.4 actin molecules per 40-kD fragment. The data are normalized to percent of maximum binding given by fluorescence/maximum fluorescence for each sample and are plotted versus the number of actin molecules added per protein. ○, brevin plus 0.2 mM $CaCl_2$; ●, are for brevin plus 2 mM EGTA. The corresponding 40-kD data are given (△ and ▲). The brevin plus EGTA data were calculated using the maximum fluorescence value obtained for brevin plus Ca^{2+}. Sample additions were made and fluorescence measurements taken after 15–20 min at 20°C.

actions in the presence or absence of Ca^{2+}, using either 0.1 M sodium phosphate, pH 7.0 or 0.15 M NaCl, 10 mM Tris-HCl, pH 7.5. Fig. 7*b* illustrates the results using CT40. We find complex formation in both Ca^{2+} and EGTA and have estimated the stoichiometry of binding by estimating the Stokes radius of the complex by comparison of the elution time with elution times for proteins of known Stokes radii. The Stokes radius of the CT40–actin complex is that expected for a protein of ~125,000 mol wt. In four separate determinations the range of values was 125,000–135,000, which indicates that there are two actin molecules bound to one CT40 fragment. This complex is formed in either Ca^{2+}- or EGTA-containing buffers.

Discussion

The data show that the brevin molecule is organized into two approximately equal size domains that are separated by a protease-sensitive region. The conformation of the protease-sensitive region is Ca^{2+} sensitive and is about 10-fold more accessible to either subtilisin or chymotrypsin when brevin is liganded with Ca^{2+}. Both chymotrypsin and subtilisin release a 40-kD fragment that protein sequencing places on the amino terminal half of the molecule. The reconstitution studies and fluorescence measurements show that the 40-kD fragment contains both actin binding sites. The Ca^{2+}-sensitive epitopes recognized by the monoclonal antibodies are on the carboxyl half of the molecule, and from the immunoblot data we have concluded that the 8G5 epitope is on a 20-kD fragment near the carboxyl terminal. The actin binding domain is defined by retention on DNAse I–agarose as a complex with actin, by its ability to increase the fluorescence of NBD–G-actin, and by its severing, capping, and nucleating activities. The Ca^{2+} regulatory domain is defined by two conformation specific monoclonal antibodies that do not react with the actin binding fragment.

The fact that the actin binding domain retains a significant fraction of its severing, capping, and nucleation activities, but is unaffected by Ca^{2+}, shows that Ca^{2+} binding is not required to induce a brevin conformation that will interact with actin. The reverse appears to be the case, the 40-kD fragment appears to have constitutive severing and capping activity that is inhibited in the whole molecule at low Ca^{2+} concentrations. Ca^{2+} binding appears to induce a conformation change that makes these binding sites accessible to actin. Cleavage with subtilisin separates the actin binding domain from the inhibitory Ca^{2+} regulatory domain and also makes these sites accessible.

Kwiatkowski et al. (12) have reported on the isolation of actin binding domains from brevin using chymotrypsin digestion. They have focused on CT17, a 17K fragment from the amino terminal end of the brevin molecule, that binds to G-actin–agarose and retains ~1% of the severing activity. We assume, but have not specifically demonstrated, that this is the 15–17-kD fragment that appears later in our chymotrypsin digests. We have isolated a similar 17-kD fragment from trypsin digests that retains severing activity and have used monoclonal antibodies to show this comes from the amino terminal of the 40-kD fragment. Kwiatkowski et al. (12) also describe a set of internal peptides, CT52 and CT47, that bind to G-actin in Ca^{2+}, but not EGTA, and CT47 has no severing, capping, or nucleating activity. We see no similar major actin-binding fragments in our chymotrypsin digests and note that the 45-kD fragments from the carboxyl half of the molecule do not interact with actin.

In Fig. 8, we have diagrammed the organization of the various peptides. We have defined the order of the two Ca^{2+} sites by the following observations. CT40 and S40 are located at the N-terminus and do not react with either antibody. S45/43 and CT45/43 contain both epitopes. The cleavage product, U75, from an unknown protease, in some of our brevin

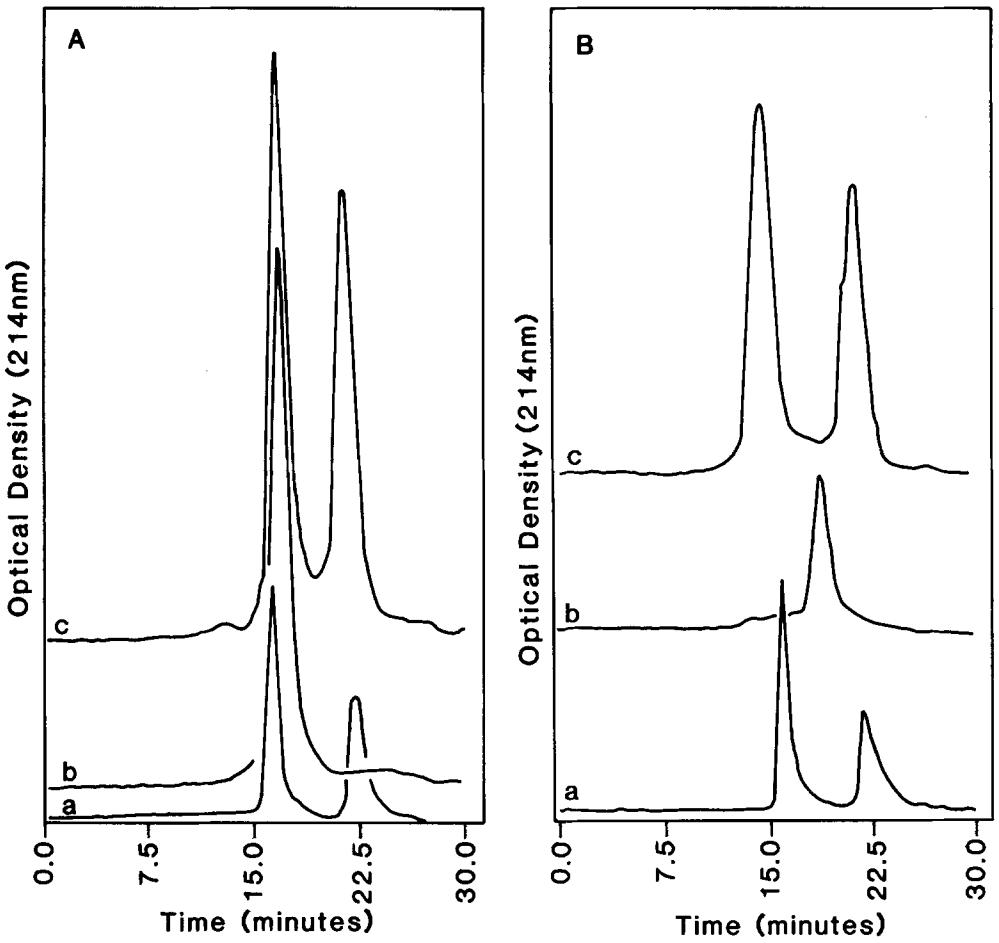

Figure 7. Formation of actin-brevin fragment complexes. G-actin at a final concentration of 0.2 mg/ml was mixed with either the 45-kD carboxyl terminal fragment at a final concentration of 0.2 mg/ml (*a*) or the 49-kD amino terminal fragment at a final concentration of 0.2 mg/ml (*b*) and incubated for 5 min at 20°C. 25-μl samples of the 2:1 actin/fragment mixtures were injected onto a Waters I 125 column in tandem with a Waters 300 SW column equilibrated with 0.1 M sodium phosphate at pH 7.0. The flow rate was 1.0 ml/min at 20°C. In each panel, curve *a* is from the G-actin standard. The peak at ~16.5 min is G-actin, the second peak at 22.5 min is from ATP. Curve *b* is for either the 45-kD fragment (panel *a*) or the 40-kD fragment (panel *b*). The *c* curves are for the mixtures. There is no shift in elution position for the actin + 45-kD mixture, but the actin + 40-kD mixture gives a more rapidly eluting complex with a larger Stokes radius and an apparent molecular weight of 125,000 when compared with standard proteins of known Stokes radius and molecular weight. Four determinations gave a range of 125,000–135,000-mol-wt. We see the same result with the 40-kD fragment + actin in the presence of 2 mM EGTA. The optical densities at 214 nm are arbitrary and have been scaled to allow the curves to be placed over one another. Similar results were obtained using 10 mM Tris-HCl, 150 mM NaCl, 0.2 mM $CaCl_2$, pH 7.5 as the equilibrating buffer with and without 2 mM EGTA. In this buffer, however, we find that brevin interacts to some degree with the resin in the separating columns.

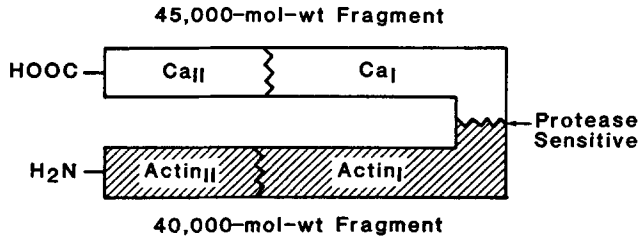

Figure 8. Diagram of brevin functional domains. This is a schematic representation of the functional domains of the brevin molecule. The arrows indicate sites of protease sensitivity for chymotrypsin, subtilisin, and an unknown protease. Sequencing places the 40,000-mol-wt fragment with severing/capping activity at the amino terminal. We locate Ca site II, the exchangeable Ca^{2+} site, on the carboxyl terminal using the 8G5 IgG monoclonal antibody that binds to brevin and gelsolin or their corresponding actin complexes only if Ca^{2+} is present. Ca site I, the non-exchangeable site in gelsolin–actin and brevin–actin complexes, was located using the 4F8 IgA monoclonal antibody that binds to brevin–actin complexes even in EGTA. We have ordered actin sites I and II arbitrarily and propose that actin site I is located close to Ca site I. Furthermore, we infer that Ca site II and actin site II must be folded into close proximity if the carboxyl portion of the molecule is to inhibit severing in the absence of Ca^{2+}.

preparations, reacts with 4F8 IgA, but not 8G5 IgG. This places at least part of the 8G5 epitope, within 18–20 K of the C-terminus. Using functional criteria, 8G5 appears to be associated with Ca site II, the exchangeable Ca^{2+} binding site (9). The non-exchangeable site, Ca site I, must be nearer the center of the molecule and is clearly placed on CT45/43. On immunoblots, CT45/43 reacts strongly with 4F8 IgA. We cannot unequivocally decide which actin binding site corresponds to site I, the non-exchangeable site. On the basis of proximity to the 4F8 epitope, we suggest that the interior actin binding site corresponds to site I.

We infer that Ca site II and actin site II must be in close proximity if the carboxyl part of the molecule is to inhibit actin–brevin interactions in the absence of Ca^{2+}. In support of this, we have preliminary evidence that the 75,000-mol-wt fragment, U75, missing only Ca site II, actively severs filaments in EGTA. Finally, we have some evidence that a 70,000–75,000-mol-wt trypsin fragment, missing only the amino terminal, will cap but not sever filaments.

The authors wish to thank Robyn Lin for excellent technical assistance and Brenda Cipriano for expert help in preparing the manuscript.

This work was funded by National Institutes of Health grants GM26091 and HL26973 to J. Bryan.

Received for publication 15 October 1985, and in revised form 27 December 1985.

References

1. Bradford, M. M. 1976. A rapid and sensitive method for the quantitation of microgram quantities of protein utilizing the principle of protein-dye binding. *Anal. Biochem.* 72:248–254.

2. Bryan, J., and L. M. Coluccio. 1985. Kinetic analysis of F-actin depolymerization in the presence of platelet gelsolin and gelsolin-actin complexes. *J. Cell Biol.* 101:1236–1244.

3. Bryan, J., and M. C. Kurth. 1984. Actin-gelsolin interactions: evidence for two actin-binding sites. *J. Biol. Chem.* 259:7480–7487.

4. Doi, Y., and C. Frieden. 1984. Actin polymerization. The effect of brevin on filament size and rate of polymerization. *J. Biol. Chem.* 259:11868–11875.

5. Harris, H. E., J. R. Bamburg, and A. G. Weeds. 1980. Actin filament disassembly in blood plasma. *FEBS (Fed. Eur. Biochem. Soc.) Lett.* 121:102–114.

6. Harris, H. E., and J. Gooch. 1981. An actin depolymerizing protein from pig plasma. *FEBS (Fed. Eur. Biochem. Soc.) Lett.* 123:49–53.

7. Harris, D. A., and J. H. Schwartz. 1981. Characterization of brevin, a serum protein that shortens actin filaments. *Proc. Natl. Acad. Sci. USA.* 78:6798–6802.

8. Harris, H. E., and A. G. Weeds. 1983. Plasma actin depolymerizing factor has both calcium-dependent and calcium-independent effects on actin. *Biochemistry.* 22:2728–2741.

9. Hwo, S., and J. Bryan. 1986. Immuno-identification of Ca^{2+}-induced conformational changes in human gelsolin and brevin. *J. Cell Biol.* 102:227–236.

10. Kilhoffer, M., and D. Gerard. 1985. Fluorescence study of brevin, the M_r 92,000 actin-capping and -fragmenting protein isolated from serum. Effect of Ca^{2+} on protein conformation. *Biochemistry.* 24:5653–5660.

11. Kurth, M. C., L.-L. Wang, J. Dingus, and J. Bryan. 1983. Purification and characterization of a gelsolin-actin complex from human platelets: evidence for Ca^{2+}-insensitive functions. *J. Biol. Chem.* 258:10895–10903.

12. Kwiatkowski, D. J., P. A. Janmey, J. E. Mole, and H. L. Yin. 1985. Isolation and properties of two actin-binding domains in gelsolin. *J. Biol. Chem.* 260:15232–15238.

13. Laemmli, U. K. 1970. Cleavage of structural proteins during the assembly of the head of bacteriophage T4. *Nature (Lond.).* 227:680–685.

14. Markey, F., T. Persson, and U. Lindberg. 1982. A 90,000-dalton actin-binding protein from platelets comparison with villin and plasma brevin. *Biochim. Biophys. Acta.* 709:122–133.

15. Norberg, R., R. Thorstensson, G. Utter, and A. Fagraeus. 1979. F-actin-depolymerizing activity of human serum. *Eur. J. Biochem.* 100:575–583.

16. Spudich, J. A., and S. Watt. 1971. The regulation of rabbit skeletal muscle contraction. *J. Biol. Chem.* 246:4866–4871.

17. Tellam, R., and C. Frieden. 1982. Cytochalasin D and platelet gelsolin accelerate actin polymer formation. A model for regulation of the extent of actin polymer formation in vivo. *Biochemistry.* 21:3207–3214.

18. Thorstensson, R., G. Utter, and R. Norberg. 1982. Further characterization of the Ca^{2+}-dependent F-actin-depolymerizing protein of human serum. *Eur. J. Biochem.* 126:11–16.

19. Towbin, H., T. Staehlin, and J. Gordon. 1979. Electrophoretic transfer of proteins from polyacrylamide gels to nitrocellulose sheets: procedure and some applications. *Proc. Natl. Acad. Sci.* 76:4350–4355.

20. Wang, L.-L., and J. Bryan. 1981. Isolation of calcium-dependent platelet proteins that interact with actin. *Cell.* 25:637–649.

21. Yin, H. L., J. H. Hartwig, K. Maruyama, and T. P. Stossel. 1981. Ca^{2+} control of actin filament length. Effects of macrophage gelsolin on actin polymerization. *J. Biol. Chem.* 256:9693–9697.

22. Yin, H. L., D. J. Kwiatkowski, J. E. Mole, and F. Sessions-Cole. 1984. Structure and biosynthesis of cytoplasmic and secreted variants of gelsolin. *J. Biol. Chem.* 259:5271–5276.

23. Yin, H. L., and T. P. Stossel. 1979. Control of cytoplasmic actin gel-sol transformation by gelsolin, a calcium-dependent regulatory protein. *Nature (Lond.).* 281:583–586.

24. Yin, H. L., and T. P. Stossel. 1980. Purification and structural properties of gelsolin, a Ca^{2+}-activated regulatory protein of macrophages. *J. Biol. Chem.* 19:9490–9493.

25. Yin, H. L., K. S. Zaner, and T. P. Stossel. 1980. Ca^{2+} control of actin gelation: interaction of gelsolin with actin filaments and regulation of actin gelation. *J. Biol. Chem.* 19:9494–9500.